Acta Cryst. (1987). A43, 677-683

Ytterbium L_{III}-Edge Anomalous Scattering Measured with Synchrotron Radiation Powder Diffraction

BY G. WILL,* N. MASCIOCCHI,† M. HART‡ AND W. PARRISH

IBM Research, Almaden Research Center, 650 Harry Road, San Jose, California 95120-6099, USA

(*Received 6 October* 1986; *accepted 7 April* 1987)

Abstract

The use of synchrotron powder diffraction patterns to determine anomalous scattering contributions is described. The method is illustrated by the determination of f' of Yb at the Yb L_{III} absorption edge. Four data sets were collected with four wavelengths, fitted with Gaussian profiles and the integrated intensities used to determine by least-squares methods the crystal-structure parameters and the real part f' of the anomalous dispersion. The derived f' values had a precision of ±0·2 electron units and averaged 32% higher than the Cromer-Liberman theoretical values.

Introduction

Near the absorption edges, when the energy of X-rays becomes comparable to the absorption levels of the atoms in the crystal, the scattering is affected in amplitude as well as in phase. This effect, known as anomalous X-ray scattering, is well known as a powerful tool for estimating the phases in crystal structure analysis (Ramaseshan & Abrahams, 1975). The method is presently used mainly in macromolecular and protein structure determinations, where rare-earth atoms showing large anomalous scattering effects at their L edges are especially well suited (Phillips & Hodgson, 1980).

The use of the method for phase determination requires the selection of wavelengths close to an absorption edge. Measurements at several wavelengths are advisable. In the past, this requirement could not be met, because of the few characteristic wavelengths available from X-ray tubes. The situation has been changed with synchrotron radiation sources, which are characterized by a high-intensity broad continuous energy spectrum up to high energies and provide a unique opportunity to use a monochromator to select any wavelength suitable for anomalous scattering. Knowledge of the values of the anomalous scattering factors at these wavelengths for the elements chosen is essential.

Relativistic calculations of the anomalous scattering factors were published by Cromer & Liberman (1970, 1981). However, these calculations generally do not show sufficient agreement with experimental data for the L absorption edges. Despite corrections and improvements of the theory (Cromer, 1983; Liberman, 1986), there are still systematic differences between measured values and those calculated. The inadequacy of this theoretical model near the L absorption edge is evident and therefore these terms have to be determined experimentally.

The best method is probably the direct determination from refractive-index measurements with an X-ray interferometer (Begum, Hart, Lea & Siddons, 1986). Their measurements of f' agreed with the Cromer & Liberman theoretical values to within 0·5 electron units for the K absorption edges. Hoyt, de Fontaine & Warburton (1984) used EXAFS (extended X-ray absorption-edge fine structure) to determine f'' from the absorption spectra of Cu, Ni and Ti, and calculated f' by the Kramers-Kronig integral. Suortti, Hastings & Cox (1985) used synchrotron radiation to determine f' for Ni with a pure Ni powder sample. They made accurate absolute integrated intensity measurements of three reflections at several wavelengths above the Ni K absorption edge and their values were stated to be in very close agreement with interferometer values and those calculated from absorption coefficients. Such experiments depend entirely on the precise determination of scale constants, which is an exceptionally skilled process. This is avoided in the method described below.

The direct derivation from X-ray diffraction crystal-structure measurements using the wavelength selectivity provided by synchrotron radiation is a very reliable method. For example, single-crystal methods were used for the three L absorption edges of Cs and the K edge of Co (Templeton, Templeton, Phillips & Hodgson, 1980) and the L edges of Gd and Sm (Templeton, Templeton, Phizackerley & Hodgson, 1982). Crystals with well determined crystal structures are selected and the scale factor and the dispersion terms determined by least-squares methods. A full

* Permanent address: Mineralogical Institute, University of Bonn, Bonn, Federal Republic of Germany.

† Permanent address: Istituto di Strutturistica Chimica Inorganica, Università di Milano, Italy.

‡ Permanent address: Department of Physics, The University, Manchester M13 9PL, England.

0108-7673/87/050677-07$01.50

data set of several hundred reflections must be measured for each wavelength.

Powder method

Equivalent powder diffraction experiments, such as the prototype described in this paper, relinquish the opportunity to measure polarization-dependent phenomena but have the advantage of simplicity over single-crystal methods in the determination of some scalar parameters. Crystal structure information can now be obtained with considerable confidence and precision from synchrotron-radiation powder data. Because of the overlaps in powder diffraction patterns, it is advisable to use simple compounds with well determined structures. In our present experiments, we used 99·9% Yb_2O_3 powder. The oxygen serves as an 'internal standard' so that the absolute scale factor is totally independent of the f' value determined in any statistical analysis. The use of simple structures containing oxygen (or another element) is an important factor in deriving dependable values. The procedures for anomalous scattering studies are basically the same as for single crystals (Templeton *et al.*, 1980, 1982) and are described below.

Data were collected with four wavelengths slightly longer than the Yb L_{III} absorption edge defined in Fig. 1. The integrated intensities were derived from a double Gaussian profile-fitting function and used in a powder least-squares refinement program (*POWLS*) for structure refinement and determination of f'. The method has been used successfully with other profile-fitting functions to refine data obtained with X-ray tube focusing (Will, Parrish & Huang, 1983) and synchrotron-radiation parallel-beam diffractometry (Will, Masciocchi, Parrish & Hart, 1987).

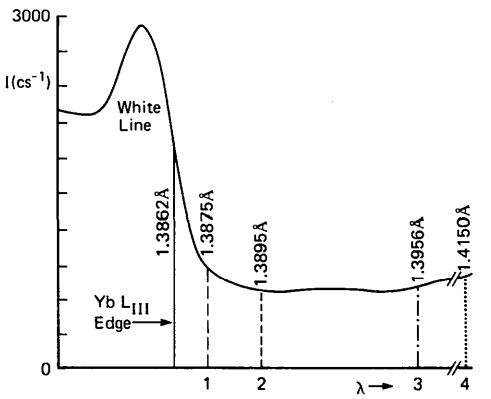

Fig. 1. Spectrum in vicinity of Yb L_{III} absorption edge obtained with energy-dispersive diffraction and Yb_2O_3 powder sample. The 'white line' convolved with the Si(111) resolution function is approximately 9·6 eV wide at half height. The four wavelengths used are indicated by the dashed lines.

The absorption changes rapidly in the vicinity of the absorption edge and is very large on the short-wavelength side. This causes difficult problems in single-crystal measurement where accurate absorption corrections as a function of λ and 2θ are required. An important advantage of the symmetrical powder diffractometer geometry used in this experiment is that the incident and reflected rays make the same angle to the powder specimen surface at all values of 2θ. The integrated intensities are proportional to $1/\mu$ where μ is the linear absorption coefficient of the specimen and are independent of θ so that no absorption corrections are required for the relative intensities.

Synchrotron radiation has several advantages: (1) Any desired wavelength can be selected close to the absorption edge. (2) The high intensity of the synchrotron beam allows good counting-statistical precision and fast data collection at several wavelengths. (3) Owing to the small beam divergence, together with the parallel-slit geometry used, the resolution and peak-to-background ratio are very good in the entire pattern, as shown in Fig. 2. (4) The simple symmetrical profiles simplify the profile-fitting procedure.

In this communication, we report the method and the results obtained on ytterbium determined from a Yb_2O_3 sample. Powder diffraction data measured at four wavelengths were used to determine the values of f', the correction term for the real part in the scattering factor of Yb at the L_{III} absorption edge.

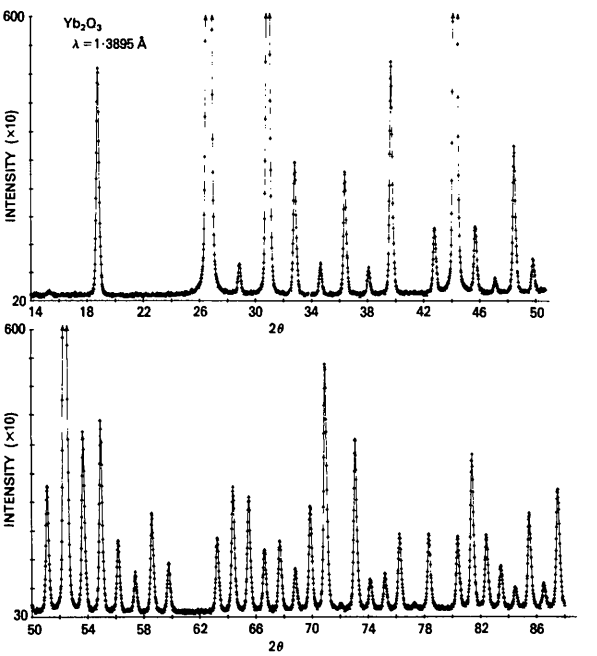

Fig. 2. Synchrotron powder diffraction pattern of Yb_2O_3, resolution 0·17°, λ = 1·3895 Å. The highest peak intensity was 56 600 counts s^{-1} (222) at 26·7°.

Owing to the intrinsic overlaps of the Friedel pairs (hkl) and $(-h,-k,-l)$ in powder diagrams, the imaginary term f'' cannot be derived from the intensities. However, if f'' is of interest, it can be calculated from f' by the Kramers–Kronig dispersion relation.

Experimental

The experiments were performed at the Stanford Synchrotron Radiation Laboratory (SSRL) with an Si(111) channel monochromator and parallel-slit geometry (Parrish & Hart, 1985). The monochromator was made from a dislocation-free silicon ingot which gave high intensity and virtually no harmonic content when used with a single-channel pulse-height analyzer. The energy resolution of the monochromator (Beaumont & Hart, 1974) is determined by two contributions, the energy spread of the perfect-crystal bandpass, $1{\cdot}33\times10^{-4}$ for Si(111), and the usual contribution from the beam divergence cot $\theta\Delta\theta$ which was of similar magnitude at large scattering angles and small at low scattering angles. The angular range in the experiments reported here was arbitrarily limited to $2\theta = 14$–$88°$ yielding 44–48 well resolved peaks from 101 planes including many intrinsic overlaps (planes occurring at exactly the same 2θ reflection angle and having the same $N = h^2+k^2+l^2$ but with different integers or sequence of integers). The step-scanning was done with $\Delta 2\theta = 0{\cdot}02°$ and 1 s count time at each step. The peak intensity of the highest peak (222) was 56 600 counts s^{-1}. The 3700 points required about 1·2 h per run. The monochromator intensity was monitored by measuring the scattering from a 0·05 mm thick beryllium foil inclined 45° to the beam and data were averaged over each 100 steps. The monitor intensity declined smoothly with the decreasing ring current during the period of these runs.

The wavelengths were determined by a modified energy-dispersive-diffraction (EDD) method in which the monochromator is step-scanned and the Yb_2O_3 specimen and scintillation counter remain in a fixed $\theta:2\theta$ relation (Parrish & Hart, 1985). One wavelength is measured at a time and is increased with each monochromator step. The resolution is determined by the diffractometer geometry rather than by a solid-state detector as used in conventional EDD. There is some uncertainty as to which feature of the edge to select and we associated the point shown in Fig. 1 with the Yb L_{III} absorption edge, $\lambda = 1{\cdot}3862$ Å (Bearden, 1964). The four wavelengths used for the powder diffraction patterns were arbitrarily selected and their values determined with respect to the absorption-edge wavelength as defined above.

The samples were prepared by mixing the Yb_2O_3 powder with collodion–amyl acetate binder and packed in a 25·4 mm diameter cylindrical aluminium holder. After drying, the surface was scraped flat and made normal to the rotation axis. The 1 mm thickness was totally absorbing for the wavelengths used.

The specimen must be very carefully prepared for precision X-ray studies. The preparation problems are mitigated with large samples as in neutron diffraction, or with wide beam divergence as in laboratory-focusing X-ray geometries, but it is particularly difficult in parallel-beam diffractometry where the angular range of particles oriented to reflect is much smaller (Parrish, Hart & Huang, 1986). It is necessary to use small particles and to rotate the specimen at 50 to 150 revolutions min^{-1} around the axis normal to the surface to obtain reliable intensities.

The particles should be neither too small to avoid excessive profile broadening, nor too large to avoid gross errors. The range 1–10 μm appears to be satisfactory. Somewhat smaller particles can be used for simple high-symmetry structures where the resultant line broadening causes no problems with overlapping reflections (other than the intrinsic overlaps). The average particle size of the Yb_2O_3 powder used was 380 Å, determined from profile broadening by the Scherrer equation. We also constructed a device to oscillate the specimen simultaneously during the rotation but the results have not yet been evaluated.

In addition to the methods described above, it is necessary to include a term GP in the structure refinement to correct the observed relative intensities for the 'preferred orientation'.

$$I_{calc}(\text{corr}) = I_{calc}\exp\left[-\text{GP}\times\varphi^2\right] \qquad (1)$$

where φ is the acute angle between the diffraction plane and a selected preferred orientation plane. It is not safe to assume that the morphological features of the macrocrystals determine the preferred orientation plane. The *POWLS* program was modified to carry out a fast seven-cycles least-squares refinement to determine R(Bragg) systematically by use of each of the first 15–20 permissible Miller planes as a preferred orientation plane. The calculation takes only one second of CPU time and the plane which gave the smallest R(Bragg) was selected as the preferred orientation plane. The intensity corrections were between 0 and 3·6% and in the worst case, the $h00$ reflections with $\varphi(111/h00) = 54{\cdot}74°$, the correction reached 5·1%.

Profile analysis and crystal structure refinement

Yb_2O_3 crystallizes in space group $Ia3$-T_h^7. Because of the tetrahedral character of point group T, $F(hkl) = F(klh) = F(lhk)$, but $\neq F(khl)$. These reflections are marked with an asterisk in Table 1, and superimposed reflections with the same N but different integers are shown by daggers. The structure

Table 1. *Observed and calculated integrated intensities for* $\lambda = 1{\cdot}3895$ Å

N	hkl	d(Å)	I(obs)	I(calc)
4	200	5·2180	271	266
6	211	4·2605	11 764	11 968
8	220	3·6897	15	22
12	222	3·0126	123 538	123 580
14*	321	2·7891	1128	1161
16	400	2·6090	36 568	36 426
18	411	2·4598	6649	6619
20*	420	2·3336	1479	1401
22	332	2·2250	6201	6196
24	422	2·1302	1152	1135
26*	431	2·0467	11 586	11 259
30*	521	1·9053	n.a.	2660
32	440	1·8448	54 751	54 613
34	433	1·7998	3247	3251
36	442†	1·7393	460	602
38	532†	1·6929	7281	7436
40	620	1·6501	1389	1627
42*	541	1·6103	5713	5965
44	622	1·5733	43 428	43 839
46*	631	1·5387	8755	8672
48	444	1·5063	9300	8790
50*	543	1·4759	3350	3289
52*	640	1·4472	1731	1790
54*	552†	1·4202	4831	4781
56	642	1·3946	2702	2331
62	732†	1·3254	3697	3572
64	800	1·3045	6288	6282
66*	554†	1·2846	5958	5856
68*	644†	1·2656	3077	3002
70*	653	1·2473	3577	3618
72	822†	1·2299	1983	2021
74*	743†	1·2132	5439	5546
76	662	1·1971	12 691	12 483
78*	752	1·1816	150	183
80*	840	1·1668	8566	8837
82	833	1·1525	1493	1612
84*	842	1·1387	1715	1764
86*	761†	1·1253	3870	3859
88	664	1·1125	170	232
90*	754†	1·1001	3911	3871
94*	932†	1·0764	3700	3648
96	844	1·0651	8156	7923
98*	853†	1·0542	3705	3807
100*	860†	1·0436	2125	2256
102	772†	1·0333	1072	1123
104*	862†	1·0233	5077	5041
106*	943	1·0136	1172	1289
108	666†	1·0042	6646	6847

* Indicates reflections with the same hkl triplet, but which, owing to the tetrahedral character of the point group, have differences in intensities between $I(hkl)$ and $I(khl)$.

† Indicates intrinsically overlapping reflections with the same $N = h^2+k^2+l^2$, but different integers.

type is α-Mn_2O_3 with the following atomic positions:

Yb(1):	8 (b)	$\frac{1}{4}$	$\frac{1}{4}$	$\frac{1}{4}$
Yb(2):	24 (b)	x	0	$\frac{1}{4}$
O:	48 (l)	x	y	z.

The lattice parameter was determined from least-squares refinement and the average of the four runs was 10·436(1) Å.

The integrated intensities were determined by profile fitting the individual peaks and were used in the *POWLS* program for least-squares refinement (Will, 1980). There is no universal profile-fitting function and none of the following were satisfactory: single Gaussian, sum of Lorentzians, Pearson VII and pseudo-Voigt. The best fitting function was achieved by superimposing two Gaussian functions with a 1:2 ratio of the FWHM and the peak height. The goodness of fit

$$R(\mathrm{PF}) = \left\{ \frac{\sum_{i=1}^{n} [Y_i(\mathrm{obs}) - Y_i(\mathrm{calc})]^2}{\sum_{i=1}^{n} Y_i(\mathrm{obs})^2} \right\} \times 100\% \qquad (2)$$

ranged from 1 to 2·5% for all the Yb_2O_3 peaks. A typical profile-fitted section is shown in Fig. 3 where the differences of observed and calculated points are shown at half height on the same intensity scale. The shapes were constant and the widths increased with 2θ owing to particle-size broadening and wavelength dispersion. The rapid decay of the tails and the relatively large peak separations were advantageous in deriving good intensity data.

At the outset of this investigation, we added a cosine modulation term to a single Gaussian with about a 2% contribution to the integrated intensity or about 12% in the peak center, which gave only slightly less agreement (Will, Masciocchi, Parrish & Hart, 1987). Data sets 1, 3 and 4 were handled this way. This method was abandoned in favor of the simpler double Gaussian for data set 2, which gave slightly better agreement between observed and calculated intensities, as was also reflected in the better R(Bragg) value. The parameters, especially the f' values, were not affected. Background refinement was included in both procedures.

The experimental data had 45–48 fitted peaks, depending on the wavelength. The integrated intensity data from the profile fitting were corrected for the smooth decline in the monochromatic

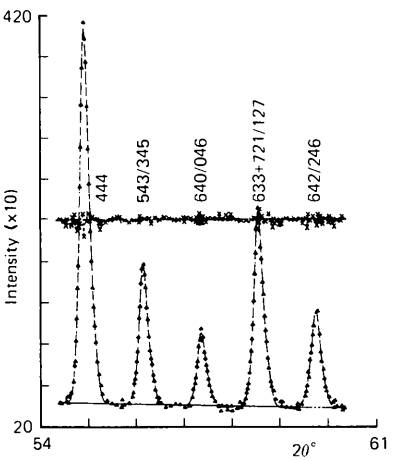

Fig. 3. Profile fitting with double-Gaussian function of five weak reflections, R(PF) = 1–2%. The observed-calculated differences are shown at one-half full ordinate height.

Table 2. *Refined structure data for* Yb_2O_3

	Wavelength (Å)			
	1·3875	1·3895	1·3956	1·4150
Data set	1	2	3	4
f'(exp)	−21·2 (2)	−19·5 (2)	−15·5 (2)	−13·7 (2)
f'(theor)	−16·41	−14·42	−12·19	−9·86
Difference	4·8	5·1	3·3	3·8
a_0		10·436 (1)* *10·4322 (5)*†		
x(Yb)	−0·0322 (1)	−0·0322 (1) *−0·03253 (4)*†	−0·0321 (1)	−0·0322 (1)
x(O)	0·3905 (11)	0·3918 (9) *−0·3910 (6)*†	0·3909 (12)	0·3912 (11)
y(O)	0·1551 (9)	0·1545 (8) *−0·1523 (6)*†	0·1556 (10)	0·1545 (9)
z(O)	0·3798 (12)	0·3805 (9) *−0·3807 (6)*†	0·3796 (13)	0·3802 (11)
B(Yb1)	0·20 (9)	0·12 (6) *−0·25*†	0·24 (8)	0·15 (6)
B(Yb2)	0·06 (5)	−0·03 (3) *−0·21*†	0·11 (4)	0·08 (3)
B(O)	0·30 (17)	0·48 (18) *0·49*†	0·28 (18)	0·24 (17)
GP‡	0·061 (10)	0·058 (8)	0·067 (10)	0·058 (8)
R(Bragg)(%)§	1·75	1·26	1·65	1·42
wR(Bragg)(%)¶	2·30	1·64 *3·52*†	2·20	1·81

* Average four wavelengths.
† Values in italics from single crystal data, Saiko *et al.* (1985).
‡ Preferred orientation plane (111), equation (1).
§ Using unit weights.
¶ Using weighting scheme; see equation (3).

primary-beam intensity by dividing them by the monitor counts.

For the refinement, we used unit weights, *i.e.* unweighted refinement, as well as a weighting scheme based on the e.s.d.'s of the counts. Weighting was applied according to $w = 1/\sigma^2$ with

$$\sigma = 0{\cdot}5(I_{\rm obs})^{1/2} + 100 \quad \text{for } I_{\rm obs} > 400, \qquad (3)$$

and, for weak peaks, we set $\sigma = 200$ for $I_{\rm obs} \leq 400$.

The break in the weighting assignment is based on the weakest still-visible reflection in the diagram, which was about 100 in the relative units used here. These peaks could also be analyzed by the profile-fitting program. Table 1 lists the observed and calculated integrated intensities for data set 2 (λ = 1·3895 Å) and the d values. Table 2 includes weighted as well as unweighted structure refinement residuals R(Bragg) in the form

$$R(\text{Bragg}) = \sum_{i=1}^{n} w_i |I_i(\text{obs}) - I_i(\text{calc})| \Big/ \sum_{i=1}^{n} w_i I_i(\text{obs}), \qquad (4)$$

where w is a weight factor based on the standard deviations of the observed intensities. As is generally observed the unweighted refinement gave a somewhat better R(Bragg) value.

The *POWLS* program is especially well suited to handle intrinsically superimposed diffraction peaks, as well as closely spaced overlaps not resolved by the profile fitting. In the present structure with 101 Miller planes and 48 diffraction peaks, there were no overlapping peaks but a large number of superimposed peaks with different intensities, as required by the space group, and these are indicated by an asterisk and/or a dagger in Table 1. The refinement included the positional parameters x, y, z for oxygen and x for Yb(2), as well as individual isotropic temperature factors B, a scale factor SK and a preferred orientation correction term GP [equation (1)]. The form factors of Yb^{3+} and O^{2-} were used. Neutral O-atom form factors were tested but showed no differences either in the R(Bragg) values or in the parameters.

The method is based on a good knowledge of the crystal structure parameters, which can best be derived with a wavelength where f' is small or negligible. However, it is not always possible to select the wavelength where the anomalous contribution is zero, and this was true for ytterbium. It is, therefore, advisable to start with a wavelength far from the absorption edge. Since f' has to be known for the crystal structure refinements, we varied the f' values systematically in a series of least-squares calculations until we were close to the real values of f' as shown by the lowest R factors. These values were then used to determine the crystal structure parameters x, y, z and B. At the end of the whole refinement, after the f' values had also been determined by least-squares calculations, the positional and thermal parameters were allowed to vary in alternating cycles (block refinement). The

four data sets gave results consistent in themselves, as is shown by the final results in Table 2. The differences between the four runs are well within the e.s.d.'s.

We have also included in Table 2 single-crystal data published by Saiko, Ishizawa, Mizutani & Kato (1985). They used 1011 reflections obtained from a 0·2 mm diameter crystal with Mo $K\alpha$ radiation in a full-matrix least-squares procedure. The powder data based on only 46 peaks shows good agreement with the single crystal data and a smaller R(Bragg) value. The effect of high temperatures on oxygen vacancies which distort the YbO_6 polyhedra was reported for the single crystal data. The room-temperature powder data did not show site-occupancy effects.

Anomalous dispersion

After the crystal structure was established, f' could be determined again by a least-squares method using *POWLS*. SK and GP were included in the list of variables. Because of the strong correlation between the different parameters, care was taken to arrive at reliable and consistent values. Therefore the positional parameters and temperature factors were kept constant until no further changes in f' were observed. They were included again in the refinement procedure with the positional coordinates, the temperature factors and the anomalous scattering term being alternately refined in an iterative mode (block refinement), until the parameters were stable within small boundaries. The observed correlation between the temperature factors, the scale factor and the anomalous scattering term was minimized by this block refinement. The agreement with single crystal data lends confidence that the correlation problem was properly handled. It should be noted that although f' is very dependent on wavelength, the positional parameters in the four data sets were within the e.s.d.'s for all wavelengths.

Since the measurements were made on the soft side of the absorption edge, there is no contribution from the L shell to the imaginary correlation term f''. However, there is a small contribution from the K shell which was calculated by Liberman (1986) to be $f''=3{\cdot}75$ electrons. This value was included in the structure-factor calculation. Also, we included a small correction term $f'=+0{\cdot}03$ electrons for oxygen independent of λ which, as to be expected, did not change the results, and the same was true when $f''=0{\cdot}03$ electrons was included for oxygen. We assumed f' is independent of scattering angle; and that it is invariant for K and almost so for L electrons.

The final results are shown in Table 2. The crystal-structure values derived from the four data sets are well within the error limits and, therefore, the results including the f' values can be considered reasonable and physically sound. We made an additional check by calculating boundary values, for example, setting B to different values from $B=0$ to $B=0{\cdot}6$ Å^2. This gave strict physical upper and lower limits for statistically determined values of f' and, from those values, we can set an error of about 5% for f'.

Fig. 4 shows the effect of the wavelength on the position, intensity and background for two reflections, 400 at $2\theta\simeq31°$, and 844 at $2\theta\simeq82°$. The intensity increases with increasing contributions of f', as we move away from the edge. This can be seen in the plots of the form-factor values (Fig. 5). The rate of increase is greater for higher diffraction angles, because the intensity is determined basically by the value of $f+f'=f-|f'|$ (f' has the opposite sign to f)

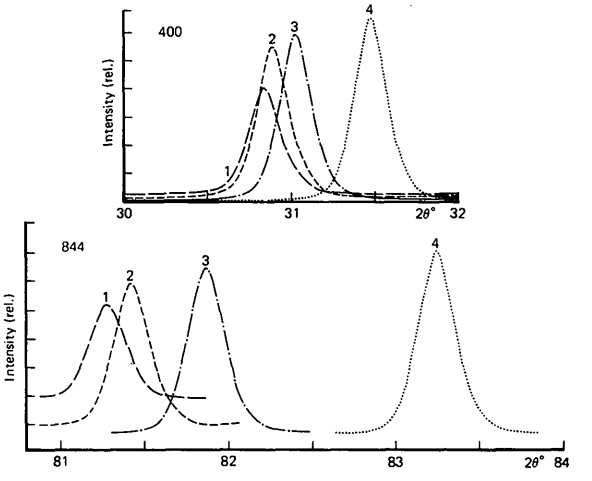

Fig. 4. Effect of wavelength on intensity and background of Yb_2O_3 400 and 844 reflections. As the wavelength decreases approaching the Yb L_{III} absorption edge, the relative intensities decrease because f' is negative and large; the fluorescence background also increases. The wavelength coding is the same as in Fig. 1.

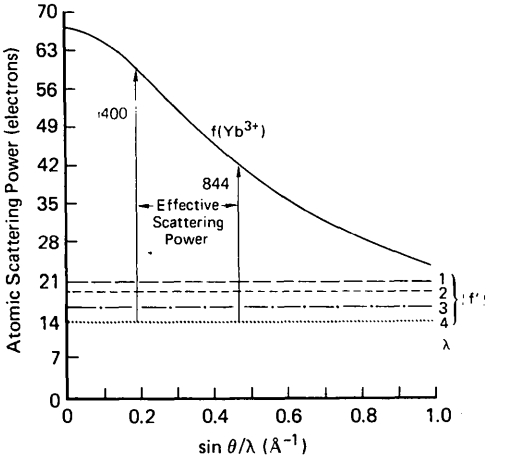

Fig. 5. The scattering factor $f(Yb^{3+})$ and the contribution of the anomalous scattering term f' which was taken to be independent of $(\sin\theta)/\lambda$. The effective scattering powers $f(\lambda)=f_0-f'(\lambda)$ are shown for $\lambda4$ for the two reflections 400 and 844. Note the wavelength increases to the right.

and also as a consequence of the strong fall-off of the form factor f with $(\sin\theta)/\lambda$. The higher background near the absorption edge, which is also clearly visible in Fig. 4, probably arises from the wavelength spread of the monochromator and harmonics (although 222 is weak) which result in some Yb L fluorescence.

Results and concluding remarks

The experimental values of the real part of the anomalous correction term f' for Yb determined from powder data analyses are 3·3 to 5·1 electron units higher than the theoretical values calculated from the Cromer & Liberman (1970, 1981) theoretical method for K and L edges. These differences are similar to those obtained for Sm and Gd using single crystal methods (Templeton *et al.*, 1980, 1982). We have made some efforts to diminish these differences and Dr Liberman tried some modifications in his program. However, at present, no agreement can be reached for the L edge and the correction terms f' have to be determined experimentally.

We have shown that synchrotron powder data can be used for anomalous scattering studies. Because single crystals with the required elements and well determined structures are not always available, simple compounds with light elements such as oxygen in polycrystalline form can be used to obtain directly the f' value at the wavelength needed for single crystal and powder structure determination.

We are indebted to the staff of the Stanford Synchrotron Radiation Laboratory for providing facilities for this research. Dr D. H. Templeton and Dr L. K. Templeton of University of California, Berkeley, kindly ran the theoretical values of f' of Yb. Dr D. Liberman of Lawrence Livermore National Laboratory discussed various aspects of the theoretical values with us. Dr M. Bellotto aided in the preparation of this manuscript.

References

BEARDEN, J. A. (1964). *X-ray Wavelengths.* USAEC Div. Tech. Inf. Ext., Oak Ridge, Tennessee, USA.
BEAUMONT, J. H. & HART, M. (1974). *J. Phys. E*, **7**, 823-829.
BEGUM, R., HART, M., LEA, K. R. & SIDDONS, D. P. (1986). *Acta Cryst.* A**42**, 456-464.
CROMER, D. T. (1983). *J. Appl. Cryst.* **16**, 437.
CROMER, D. T. & LIBERMAN, D. (1970). *J. Chem. Phys.* **53**, 1891-1898.
CROMER, D. T. & LIBERMAN, D. (1981). *Acta Cryst.* A**37**, 267-268.
HOYT, J. J., DE FONTAINE, D. & WARBURTON, W. K. (1984). *J. Appl. Cryst.* **17**, 344-351.
LIBERMAN, D. (1986). Private communication.
PARRISH, W. & HART, M. (1985). *Trans. Am. Crystallogr. Assoc.* **21**, 51-55.
PARRISH, W., HART, M. & HUANG, T. C. (1986). *J. Appl. Cryst.* **19**, 92-100.
PHILLIPS, J. C. & HODGSON, K. O. (1980). *Acta Cryst.* A**36**, 856-864.
RAMASESHAN, S. & ABRAHAMS, S. C. (1975). Editors. *Anomalous Scattering.* Copenhagen: Munksgaard.
SAIKO, A., ISHIZAWA, N., MIZUTANI, N. & KATO, M. (1985). *Yogyo Kyokai Shi*, **93**, 649-654.
SUORTTI, P., HASTINGS, J. B. & COX, D. E. (1985). *Acta Cryst.* A**41**, 413-416, 417-420.
TEMPLETON, D. H., TEMPLETON, L. K., PHILLIPS, J. C. & HODGSON, K. O. (1980). *Acta Cryst.* A**36**, 436-442.
TEMPLETON, L. K., TEMPLETON, D. H., PHIZACKERLEY, R. P. & HODGSON, K. O. (1982). *Acta Cryst.* A**38**, 74-78.
WILL, G. (1980). *J. Appl. Cryst.* **12**, 483-485.
WILL, G., MASCIOCCHI, N., PARRISH, W. & HART, M. (1987). *J. Appl. Cryst.* **20**. In the press.
WILL, G., PARRISH, W. & HUANG, T. C. (1983). *J. Appl. Cryst.* **16**, 611-622.

Acta Cryst. (1987). A**43**, 683-690

Transmission of Non-centrosymmetric Crystals by Fast Electrons in the General Laue Case

BY G. KÄSTNER

Institute of Solid State Physics and Electron Microscopy of the Academy of Sciences of the German Democratic Republic, PSF 250 Halle/S, DDR-4050 Halle, German Democratic Republic

(*Received* 24 *September* 1986; *accepted* 9 *April* 1987)

Abstract

On treating electron transmission of non-centrosymmetric crystals by the common many-beam dynamical theory, it is shown that the influence of inclined external or internal crystal boundaries as well as the influence of reflections from non-zero-order Laue zones can be treated as a convenient correction or a perturbation of the fundamental (eigenvalue) equation by means of appropriate small correction terms ε_g. Further corrections, arising from anomalous absorption, are written in a comparable form so that the two corrections can be easily compared for various conditions, mainly in kinematical or dynamical

0108-7673/87/050683-08$01.50